RSC Advances

ROYAL SOCIETY OF CHEMISTRY

www.rsc.org/advances

Cite this: DOI: 10.1039/c0xx00000x

www.rsc.org/xxxxxx

ARTICLE TYPE

Controlled synthesis of functional Ag, Ag-Au/Au-Ag nanoparticles and its nanocomposite with Prussian blue for bioanalytical applications

Prem. C. Pandey,* Richa Singh and Yashashwa Pandey

Received (in XXX, XXX) XthXXXXXXXXX 20XX, Accepted Xth XXXXXXXXX 20XX

DOI: 10.1039/b000000x

In this work, we report the facile approach to synthesize processable silver nanoparticles (AgNPs), bimetallic nanoparticles (Ag-Au/Au-Ag) decorated Prussian blue nanocomposite (PB-AgNP). The presence of cyclohexanone/formaldehyde facilitates the formation of functional AgNPs and Ag-Au/Au-Ag from 3-aminopropyltrimethoxysilane (3-APTMS) capped respective noble metal ions. The use of aforementioned reducing agents (3-APTMS and cyclohexanone) also enables the synthesis of polycrystalline Prussian blue nanoparticles (PBNPs). As synthesized PBNPs, AgNPs and Au-Ag enable the formation of nano-structured composites (PB-AgNP, PB-Au-Ag) displaying better catalytic activity than that recorded with natural enzyme. The nanomaterials have been characterized by UV-vis, FT-IR and Transmission Electron Microscopy (TEM) with following major findings: (1) 3-APTMS capped silver ions in the presence of suitable organic reducing agents [3-Glycidoxypropyltrimethoxysilane (GPTMS), Cyclohexanone and Formaldehyde] are converted into AgNPs under ambient conditions, (2) the time course of synthesis and dispersibility of the nanoparticles are found as a function of organic reducing agents, (3) the use of formaldehyde and cyclohexanone in place of GPTMS with 3-APTMS outclasses the other two in imparting better stability to amphiphilic AgNPs with reduced silanol content, (4) an increase in 3-APTMS concentrations causes decrease in nanogeometry of AgNPs, (5) simultaneous synthesis of bimetallic nanoparticles under desired ratio of silver and gold cations are recorded, (6) cyclohexanone mediated synthesis of AgNPs and Ag-Au/Au-Ag enable the formation of homogeneous nanocomposite with PBNP as peroxidase mimetic representing potential substitute of peroxidase enzyme. The peroxidase mimetic ability has been found to vary as a function of 3-APTMS concentration revealing the potential role of functional silver nanoparticles in bioanalytical applications.

Introduction

Silver nanoparticles (AgNPs) have received closer interest, especially because of their unique optical properties,[1-4] fascinating catalytic activity,[5-6] and potential applications such as

antimicrobial agent[7-9] catalysis[10] and printed electronics.[11] However, the synthesis of stabilized functional AgNPs under ambient conditions remains a challenge from following angles;[10-12] (1) stability and dispersibility in a variety of solvents, (2) processability for nanocomposite formation and (3) functional ability and biocompatibility for specific applications. Bimetallic nanoparticles (Ag-Au/Au-Ag) have been demonstrated to exhibit improved catalytic performance, because of the synergistic effect and electronic effect. Although, many experimental studies on Ag-Au/Au-Ag nanoparticles are available in literature, however, most of the them have been centred on specific applications[12-20] due to lack of dispersibility and processability in a variety of solvents. Nevertheless, advances in fine tuning of functional ability, dispersibility and processability of bimetallic nanoparticles for nanocomposite formation by controlled reaction protocol still remains a research task. Recently, biocomponent or multicomponent composite catalysts have attracted great attention [21] since loading or dispersion of catalytically active nanoparticles into the host mesoporous network results in nano-structured composites affecting the catalytic reaction process. Therefore, simple and facile approaches are needed for the synthesis of functional Ag-Au/Au-Ag with desirable size that enables the formation of nanocomposite for catalytic application. The use of reducing agents like organic amine enabled the synthesis of AuNPs having sufficient stability for practical applications.[22,23] The role of alkylchain linked to amine group has also been demonstrated to control the dispersibility of NPs in organic and aqueous media.[24] Further the functional ability of organic amine linked to alkoxysilane group[25] facilitated the synthesis of AuNPs, PdNPs, Au-Pd/Pd-Au, justifying the role of 3-APTMS for controlling nanogeometry, dispersibility, functional ability and processability in a single step[26-31]. 3-APTMS itself does not allow the formation of AuNPs, however, it facilitates rapid synthesis of metal nanoparticles in the presence of 3-APTMS compatible organic reducing agents.[26-28, 31] The micellar activity of 3-APTMS allows the use of various organic reducing agents for desired applications. In addition to that 3-APTMS and cyclohexanone also permits the synthesis of polycrystalline PBNPs.[32,33] The use of common reducing agents during synthesis of AgNPs, Ag-Au/Au-Ag and PBNPs may facilitate the formation of nano-structured composites with a crystalline framework for better catalytic applications.

Recently, the intrinsic enzyme-like activity of nanomaterials has become a growing area of interest in specific and sensitive biomolecular detection mainly due to high stability and low-cost alternative to natural enzymes.[34-37] AgNPs and its bimetallic, have been recently investigated with peroxidase-like activity.[36,38] However, in clinical diagnostics, as well in food

quality control, the required selectivity and sensitivity of the NPs as peroxidase mimetic remains an issue of research findings. The use of Prussian blue as an electrocatalyst has been demonstrated to exhibit 3 orders–of magnitude more active/selective than that of conventional catalyst in H_2O_2 reduction and oxidation in neutral media.[39] However, most of the findings are centred on the electrocatalytic properties rather than their use as peroxidase mimetic in homogeneous medium because of the insolubility of material in many solvents[40,41] Therefore, simple and facile approaches are needed for the controlled synthesis of functional PBNPs that enables the formation of nanocomposite with AgNPs/Au-Ag for catalytic applications. Recently, the controlled synthesis of processable PBNPs has been demonstrated justifying the active participation of 3-APTMS and cyclohexanone for use in both homogeneous and heterogeneous media.[32] These findings directed us to examine the possibility for the formation of nanocomposite of PBNPs and AgNPs/Ag-Au/Au-Ag in order to tune the catalytic activity even better than that of peroxidase under feasible experimental conditions. Apart from their application in homogeneous catalysis, it is also intended to understand the electrocatalytic ability of nanocomposite in heterogeneous phase as chemically modified electrode justifying the significance of as synthesized nanomaterials for wider applications. With the example of AgNPs, Au-Ag and nanocomposite of PBNPs, tailoring of peroxidase-like activity is realized by using 3-APTMS and organic reducing agents like cylohexanone/formaldehyde which introduces another effective way to regulate the synthesis and catalytic activity of NPs.

Experimental section

Chemicals

3-Aminopropyltrimethoxysilane (3-APTMS), 3-Glycidoxypropyltrimethoxysilane (GPTMS), silver nitrate ($AgNO_3$), tetrachloroauric acid ($HAuCl_4$) and *o*-dianisidine were obtained from Aldrich Chemical Co., India. Potassium ferricyanide, cyclohexanone, formaldehyde and hydrogen peroxide were obtained from Merck, India. All other chemical employed were of analytical grade.

Synthesis of Ag, Ag-Au and Au-Ag nanoparticles

3-APTMS and cyclohexanone mediated synthesis of AgNPs, Ag-Au and Au-Ag. A typical process for cyclohexanone and 3-APTMS mediated synthesis of AgNPs sol consisted of following steps: 50μL of 10 mM of $AgNO_3$ solution in methanol was premixed with 10μL of methanolic solution of 3-APTMS of desired concentrations [0.25 M for $AgNP_1$ and 0.5 M for $AgNP_2$] stirred for 2 min, followed by addition of cyclohexanone (1.9 M). The solution was kept undisturbed for 2 h. AgNPs sols of two different size ($AgNP_1$ and $AgNP_2$) of yellow colour were obtained within <3 h. The findings

on the effect of 3-APTMS and Cyclohexanone during the synthesis of AgNPs are shown in supporting information (S1). The preparation of bimetallic nanoparticles involves known ratio of metal salts. Ag-Au is made using $AgNO_3$ and $HAuCl_4$ in 4/1 ratio. The Ag-Au synthesis involves the mixing of 12µl methanolic solution of $AgNO_3$ (0.025 M) and 12 µl methanolic solution of $HAuCl_4$ (0.0025 M) under stirred condition followed by the addition of 06 µl of 3-APTMS (0.5 M) and 10µl of cyclohexanone. The reaction mixture turned purple within 2 h. Whereas Au-Ag is made using $HAuCl_4$ and $AgNO_3$ in 4/1 ratio and the synthesis involves the mixing of 12 µl methanolic solution of $HAuCl_4$ (0.025 M) and 12 µl of methanolic solution of $AgNO_3$ (0.0025 M) under stirred condition followed by the addition of 06 µl of 3-APTMS (0.5 M) and 10µl of cyclohexanone. The reaction mixture turned Dark yellow within 1 h.

3-APTMS and formaldehyde mediated synthesis of AgNPs. A typical process for formaldehyde and 3-APTMS mediated synthesis of AgNPs sol consisted of following steps: 50µL of 10 mM of $AgNO_3$ solution in methanol was premixed with 10µL of methanolic solution of desired concentration of 3-APTMS stirred for 2 min, followed by addition of formaldehyde. The reaction mixture turned Dark yellow within 30 min.

3-APTMS and GPTMS mediated synthesis of AgNPs. The typical synthesis of GPTMS and 3-APTMS stabilized AgNPs was similar as described earlier.[26,42] Methanolic suspension of 3-APTMS treated Ag^+ ions (0.025 M) was added to methanolic solution of GPTMS. The resulting mixture was stirred over a vertex cyclo mixer for 2 min. The mixture was left to stand in the dark for 12 h. After this, the colour of the sols turned to yellow indicating the formation of AgNP (I).

Synthesis of Nanocomposite of PBNPs with AgNPs and Au-Ag. PBNPs were synthesized as described earlier.[32] Nanoparticles decorated PBNP (PBNP-AgNPs and PBNP-Au-Ag) nanocomposite were prepared by careful mixing of as synthesized $AgNP_1$, $AgNP_2$, AgNP (I), Au-Ag and PBNPs. AgNPs /Au-Ag (15µl) and PBNPs (5µl) under ambient conditions and left undisturbed for 5 minutes at room temperature (25^0C).

Peroxidase-like catalytic activity of Nanocomposite. The peroxidase-like activity of as synthesized PBNP-$AgNP_1$, PBNP-$AgNP_2$, PBNP-AgNP (I) and PBNP-Au-Ag were determined spectrophotometrically by measuring the formation of the oxidized product of *o*-dianisidine at 430 nm (ε = 11.3 mM^{-1} cm^{-1}) using a Hitachi U-2900 spectrophotometer. The mimetic behaviour of nanocomposite [PBNP-$AgNP_1$, PBNP-$AgNP_2$, PBNP-AgNP (I) and PBNP-Au-Ag] was recorded in 0.1M phosphate buffer also using *o*-dianisidine at 25^0C.

Hydrogen peroxide was added to start the reaction, unless otherwise specified.

Kinetic Parameters Analysis. Steady-state kinetics was performed by varying the concentration of H_2O_2 (0–50 mM), at a fixed concentration of *o*-dianisidine. The reaction was carried out in 2 mL phosphate buffer (0.1 M, pH 7.0) and the variation of the absorbance was monitored using a spectrophotometer (Hitachi U-2900) in the time scan mode at 430 nm (ε = 11.3 mM^{-1} cm^{-1}). The kinetic parameters were calculated by fitting the absorbance data to the Michaelis–Menten equations,

$$v = V_{max}[C]/K_m + [C] \quad \text{..... [1]}$$

where v is the initial velocity, V_{max} is the maximal reaction velocity, C is the concentration of the substrate, and K_m is the Michaelis–Menten constant.

Preparation of modified carbon paste electrodes. PBNP/PBNP–AgNP (I) modified carbon paste electrode was made using electrode body (MF-3010) obtained from Bioanalytical Systems Inc. West Lafayette. The active paste having composition (w/w): PBNP/PBNP–AgNP (I) = 3 %, graphite powder = 67 %(w/w), Nujol oil = 30% (w/w) was mixed thoroughly and stored in stoppered glass vials at room temperature. The active paste was filled into well of the electrode body and the surface was manually smoothened on a clean butter paper.

Electrochemical measurements. All electrochemical measurements were performed in an electrochemical cell equipped with a three electrodes configuration having working volume of 3 mL with Electrochemical Analyzer Model CHI 830B, CH Instruments Inc. TX, USA. The working electrodes were CPE/PBNP and CPE/PBNP-AgNP (I). An Ag/AgCl reference electrode and a platinum counter electrode were used in all electrochemical measurements. The hydrogen peroxide sensing was carried out through cyclic voltammetry by scanning the potential between −0.2 to 1 V vs Ag/AgCl at the scan rate of 0.01 Vs^{-1}, in 0.1 M phosphate buffer pH 7.0 containing 0.5 M KCl.

Results and Discussion

Role of organic reducing agents during 3-APTMS mediated synthesis of AgNPs, Ag-Au and Au-Ag.

At first instant it is important to understand the significance of 3-APTMS during the synthesis of noble metal nanoparticles. Four major roles of 3-APTMS have been extensively studied for specific applications i.e.; (1) as a potential stabilizer for noble metal nanoparticles, [43-46] (2) formation of organic inorganic hybrid as catalytic material,[47] (3) in the commercial preparation of amino-silanized glass beads/surface functionalized agent having potentiality for Schiff-base linkage/carbodiimide coupling during biotechnological designs[48-50] and (4) formation of biocompatible mesoporous/nanoporous thin film of organically modified silicate.[51-58] These properties of 3-APTMS directed us to examine its role in

nanomaterial synthesis.[26-28] We have reported 3-APTMS and GPTMS mediated synthesis of AgNPs which are dispersible in aqueous media under specific composition of 3-APTMS/GPTMS ratio whereas the same is dispersible in non-aqueous media at all composition.[26,42] Such findings although, provided a novel report on the synthesis of AgNPs, but suffers a disadvantage due to increased alkoxysilane content which limits its use for many practical applications due to the formation of Si–O–Si linkage with time. Accordingly we tried to decrease the silane content by substituting other reagents in place of GPTMS. Recent reports demonstrated that the 3-APTMS itself does not enable the conversion of noble metal cations (Au^{3+}, Ag^{+} , Pd^{2+}) into respective nanoparticles, however, in the presence of suitable organic reducing agents facilitate the synthesis of the same.[28-31] Micellar nature of 3-APTMS enable controlled synthesis of NPs dispersible in various solvents as a function of organic reducing agents.[27,30,42]

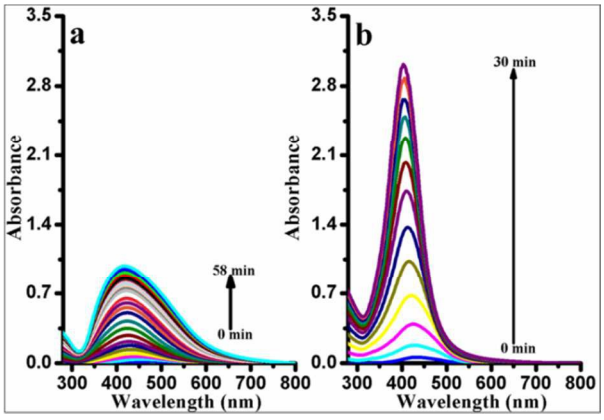

Fig. 1 Real time synthesis of AgNPs as a function of 3-APTMS concentrations [a= 0.5 M, b= 2 M] containing constant concentration of formaldehyde.

Fortunately, the choice of formaldehyde and cyclohexanone provided valuable information on the synthesis of AgNPs and its bimetallic (Ag-Au/Au-Ag) that not only decreased the silane content but also expedited the controlled formation of AuNPs, PdNPs and its bimetallic Pd–Au/Au-Pd.[24,30] The role of 3-APTMS and cyclohexanone has not been limited to noble metal NPs synthesis but also precisely enabled the synthesis of polycrystalline PBNPs,[32] revealing the potentiality of these NPs in the formation of nanocomposite. Accordingly, the role of formaldehyde/cyclohexanone on real time conversion of 3-APTMS capped silver ions has been studied. Figure 1a shows the real time synthesis of AgNPs mediated by 3-APTMS and formaldehyde at lower concentration of 3-APTMS (0.5 M), whereas Figure 1b shows the similar result at 2M APTMS. The results, as shown in Figure 1, clearly demonstrate the rapid synthesis of AgNPs as a function of 3- APTMS concentration. The higher concentration of 3-APTMS enable the complete conversion of Ag^{+} cations into AgNPs within < 0.5 h whereas, > 1 h is required at lower 3-APTMS (0.5 M) (Figure 1). Exchange of formaldehyde by cyclohexanone under similar condition again causes an increase in time of complete conversion of Ag^{+} into AgNPs i.e. 1.5-3 h. In order to understand precisely the requirement of both 3-APTMS and organic reducing agents, the formation of AgNPs under two different conditions; (1) keeping constant concentration of cyclohexanone while

changing the concentration of 3-APTMS; and (2) keeping 3-APTMS constant while changing the concentrations of cyclohexanone; are studied as shown in Supporting information S1A and S1B. The results revealed the requirement of an optimum concentration of formaldehyde /cyclohexanone for NPs synthesis (Supporting information S1C and S1D). On the other hand higher concentrations of 3-APTMS always facilitate the AgNPs formation whereas, relatively lower concentration (<0.05M) retard the same. The proposed mechanism for the 3-APTMS and cyclohexanone mediated synthesis is shown in Scheme 1:

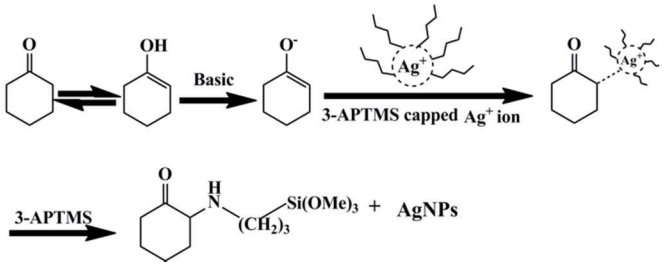

Scheme 1 Mechanism of 3-APTMS and cyclohexanone assisted synthesis of AgNPs.

Cyclohexanone in the prevailing medium undergoes keto– enol tautomerism. Enolate ion acts as an electron donor to 3-APTMS capped Ag^+ ion, which in turn acts as a Lewis acid, leading to the formation of AgNPs along with organic-inorganic hybrid (Scheme-1) as confirmed by FTIR spectra (Supporting information S2).

Both 3-APTMS and organic reducing agents control the nanogeometry of AgNPs. The TEM images of as synthesized AgNPs made from 3-APTMS and cyclohexanone at two different concentrations of 3-APTMS are shown in Figure 2 (a and d) along with SAED pattern (b and e) and particle size distribution (c and f).

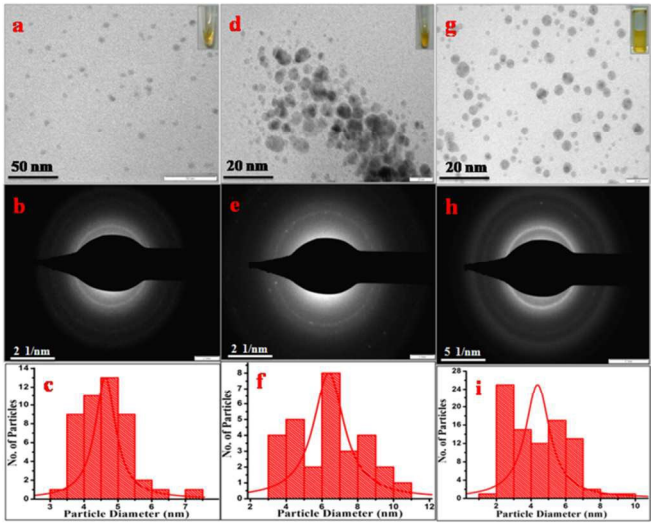

Fig. 2 TEM images of AgNPs made from the use of fixed concentration of cyclohexanone (1.9 M) and increasing concentrations of 3-APTMS (0.25 M for a, 0.5 M for d) along with respective SAED patterns (b and e) and particle size distribution (c and f); TEM images (g), SAED pattern (h) and particle size distribution (i) of AgNPs made from formaldehyde (0.8 M) and 3-APTMS (0.5 M).

The finding shows the circular nanogeometry with average size of 5 nm ($AgNP_1$) and 7 nm ($AgNP_2$) at 0.25 M and 0.5 M 3-APTMS respectively keeping constant concentration of cyclohexanone (1.9 M). The use of hydrophilic organic reducing agent like formaldehyde results homogeneous distribution of AgNPs having average particle size to the order of 4 nm as shown in Figure 2 (g) along with selected area electron diffraction (SAED) pattern (Fig.2 h) and particle size distribution (Fig.2 i). These findings reveal that an increase in 3-APTMS concentrations causes decrease in nanogeometry.[28] The question of whether the

similar reducing agents (3-APTMS and cyclohexanone) may also enable the synthesis of bimetallic nanoparticles of silver and gold was next explored.[59] The results based on UV-Vis spectroscopy on Ag-Au formation at two different ratios of Ag/Au i.e 1/4 and 4/1 are shown in Figure 3 (a) and (b) respectively that reveal the formation of bimetallic NPs.

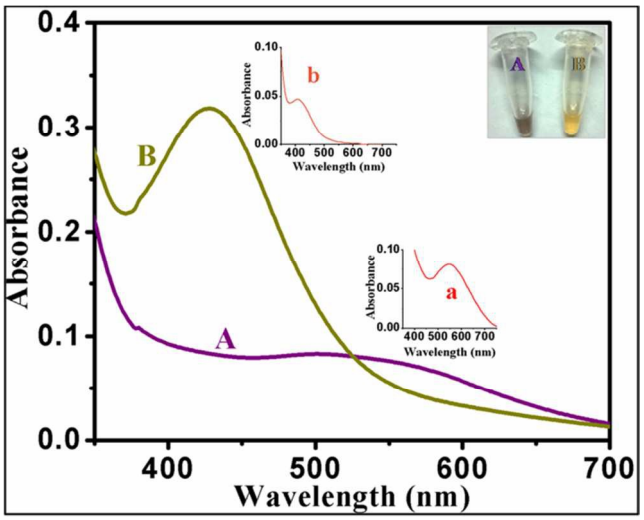

Fig. 3 UV-vis absorption spectra of Ag-Au nanoparticles made by using 3-APTMS and cyclohexanone with varying silver:gold ratio: (A) Ag-Au (1/4) and (B) Ag-Au (4/1). Inset shows the visual photographs of Ag-Au nanoparticles. UV-vis spectra of Monometallic AuNPs (a) and AgNPs (b) respectively.

The insets (a) and (b) to Figure 3 shows respective spectra for monometallic AuNPs and AgNPs respectively. TEM image of Ag-Au (1/4) nanoparticles shows circular morphology with average particle size of 10.3 nm (Figure 4a and 4b). The SAED pattern (Figure 4c) of the same clearly demonstrate the polycrystalline pattern[20,60-61] and were indexed with the (111), (200), (220), (311), (222) and (331) lattice planes with spacing 0.220 nm, 0.191 nm, 0.134 nm, 0.114 nm, 0.110 nm and 0.087 nm.

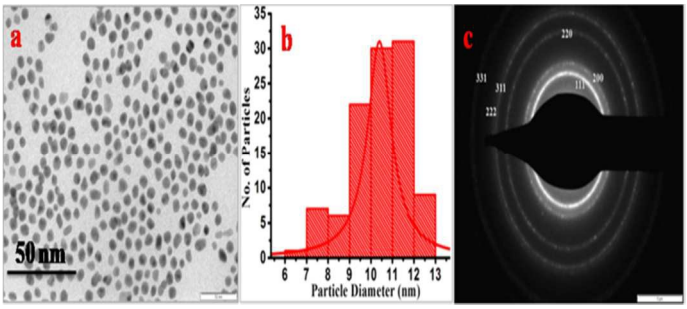

Fig. 4 TEM image (a), particles size distribution (b), and SAED pattern (c) of bimetallic Ag-Au (1/4) nanoparticles.

Effect of organic reducing agents on the dispersibility of AgNPs

The micellar behaviour of 3-APTMS and the critical micellar concentration of organic reducing agents (cyclohexanone, formaldehyde) play important role in determining the dispersibility of as synthesized nanoparticles. Dispersibility of AgNPs largely depends on the medium which in turn is determined by hydrophilic/hydrophobic behaviour of the organic moieties (formaldehyde/cyclohexanone).

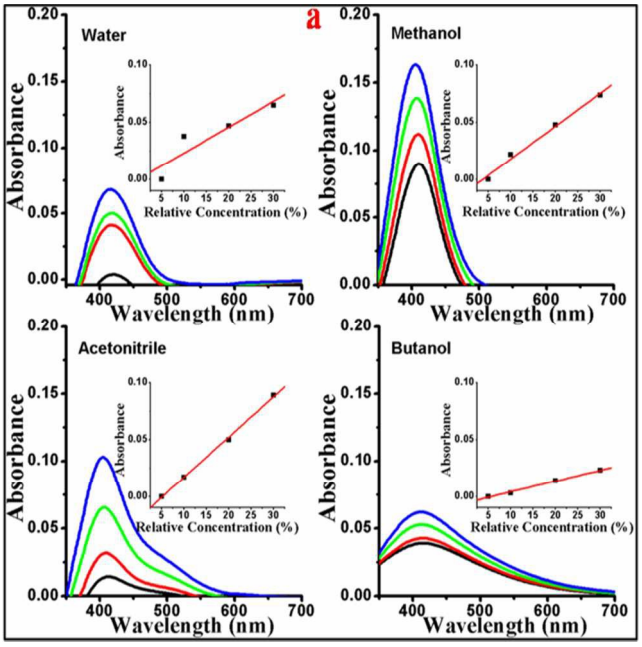

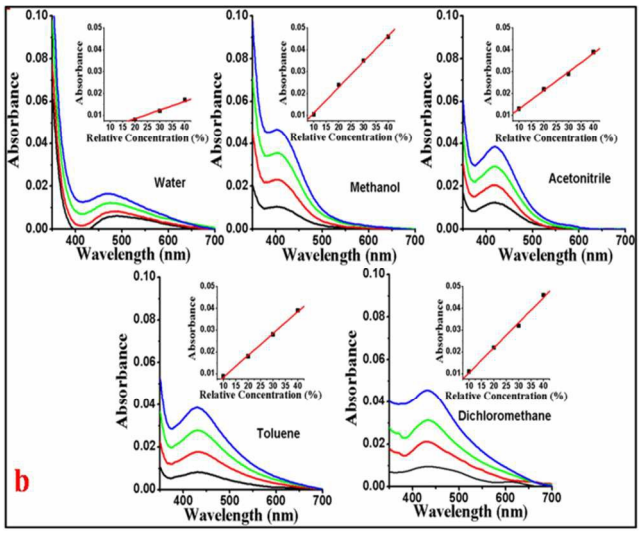

Fig. 5 (a) UV-vis absorption spectra of increasing concentrations of AgNPs made by using formaldehyde and 3-APTMS in water, methanol, acetonitrile and butanol; Respective insets show the dependence of absorption maxima (λ_{max}) on AgNPs concentration; **(b)** UV-vis absorption spectra of increasing concentrations of AgNPs made from cyclohexanone and 3-APTMS in water, methanol, acetonitrile, toluene, dichloromethane; Respective insets show the dependence of absorption maxima (λ_{max}) on AgNPs concentration.

The results on the dispersibility of AgNPs, made from 3-APTMS and formaldehyde, as a function of their concentrations in water, methanol, acetonitrile and butanol has been recorded in Figure 5a revealing linear relation between λ_{max} vs AgNPs concentrations whereas, the use of cyclohexanone (Figure 5b) facilitate the dispersibility in non-aqueous media only i.e. methanol, acetonitrile, toluene and dichloromethane.

Nanocomposite of AgNPs, Ag-Au with PBNPs. The advances in fine tuning of AgNPs/Au-Ag as biocomponent or multicomponent composite facilitate the catalytic activity of resulting nanomaterial. The use of same reducing agents while making the AgNPs/Au-Ag and functional host like PBNP may facilitate the possibility of such nanocomposite formation for catalytic application as peroxidase mimetic. Recently the role of 3-APTMS and cyclohexanone has been demonstrated in the synthesis of polycrystalline PBNP dispersion providing a suitable host matrix for nanocomposite preparation.[33] The tuning of AgNPs/Au-Ag and processable PBNP may facilitate the catalytic activity of composite material even better than that of peroxidase under feasible experimental conditions. Indeed excellent finding has been recorded on nanocomposite formation from as synthesized AgNPs/Au-Ag and PBNPs (~15.8 nm) made as described earlier.[32]

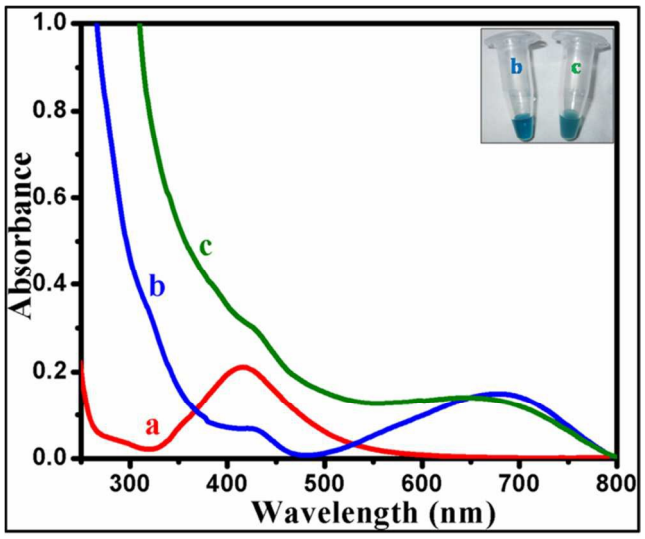

Fig. 6 UV-vis absorption spectra of AgNPs (a), PBNPs (b) and PBNP-$AgNP_2$ nanocomposite (c) made from 3-APTMS and cyclohexanone. The insets show the visual photographs of b and c.

The results on the formation of nanocomposite based on UV-vis spectroscopy are shown Figure 6. The curve-a shows the absorption spectra of AgNPs, curve-b of PBNPs whereas curve-c

represents the same for PBNP-AgNP$_2$ (Figure 6). The presence of hump at 419 nm (characteristics of AgNP) and maxima at 640 nm (characteristics of PBNP) as shown in Figure 6(c) justify the nanocomposite formation. The visual photograph of PBNP-AgNP$_2$ nanocomposite suspension as shown in inset of Figure 6(c) also revealed the tuning of AgNPs and PBNPs during nanocomposite formation. The TEM image of PBNP-AgNP$_2$ (Figure 7a and 7c) shows circular morphology with average particle size of 13 nm. The SAED pattern[62] (Figure 7b) of PBNP-AgNP$_2$ clearly demonstrates the polycrystallinity of nanocomposite and reveals the presence of AgNP and PBNP.

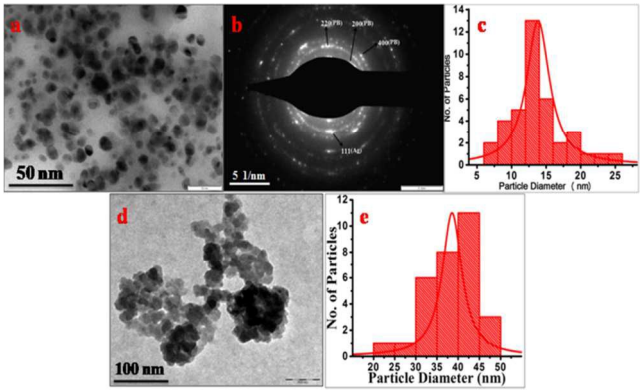

Fig. 7 TEM image (a), SAED pattern(b) and particle size distributions(c) of PBNP-AgNP$_2$ nanocomposite. TEM image (a) and particle size distributions (b) of PBNP-AgNP(I). nanocomposite.

The effect of partial tuning between AgNPs and PBNPs has also been explored. For this AgNP (I) were synthesized from 3-APTMS of same concentration and replacing cyclohexanone by GPTMS. TEM images of PBNP-AgNP (I) (Figure 7d and e) shows average particle size of 38 nm revealing tendency for agglomeration of NPs justifying the requirement of homogeneous composition of reducing agents during nanocomposite of better catalytic activity.

Peroxidase Mimetic activity of nanocomposite. The catalytic activity of nanocomposite as peroxidase mimetic was next explored. Earlier findings suggested better catalytic activity of bimetallic as compared to monometallic NPs[60] however, catalytic ability and k_m to reach the desired sensitivity remains a challenging task as compared to peroxidase enzyme for practical applications. Since PBNPs represent an excellent class of peroxidase mimetic, the nanocomposite of the same may be a suitable candidate of peroxidase replacement. Accordingly we have examined the H_2O_2 mediated oxidation of o-dianisidine in the presence of as synthesized nanomaterial as follows (Scheme 2):

$$H_2O_2 + o\text{-dianisidine}_{(red.)} \xrightarrow[PBNP\text{-}AgNP/PBNP\text{-}Au\text{-}Ag]{AgNP/PBNP/} o\text{-dianisidine}_{(ox.)} + H_2O$$

where, o-dianisidine$_{(red.)}$ and o-dianisidine$_{(ox.)}$ represent the reduced and oxidized forms of o-dianisidine. Apart from tuning of AgNPs/Au-Ag and PBNP during nanocomposite formation, another advantage of as synthesized nanomaterials is the formation of organic-inorganic hybrid between the 3-APTMS and cyclohexanone as predicted in Scheme 1. The presence of inorganic-organic hybrid facilitates the catalytic activity of nanomaterial.[46] An increase in 3-APTMS concentration during

nanoparticle synthesis enable an increase in the formation of such hybrid material and the catalytic activity as a function of 3-APTMS concentration is explored. A comparative study on the catalytic activity of AgNPs, PBNPs, PBNP-AgNP and PBNP-Au-Ag justifying the variation in absorbance at 430 nm as a function of time is shown in Figure 8 A, B, C and D respectively. The findings clearly demonstrate better catalytic activity of PBNP-Au-Ag as compared to AgNPs, PBNPs and PBNP-AgNP (Figure 8).

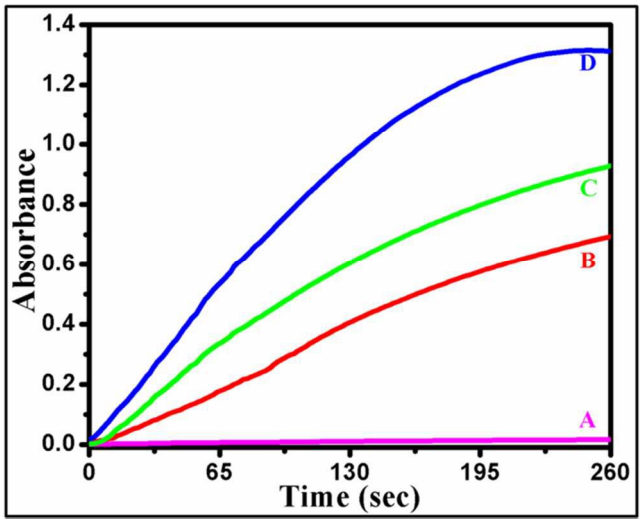

Fig. 8 Time-dependent absorbance changes at 430 nm in the presence of (A) AgNPs, (B) PBNPs, (C) PBNP-AgNP and (D) PBNP-Au-Ag nanoparticles.

. The catalytic activity of nanocomposite made with two size of AgNPs ($AgNP_1$ and $AgNP_2$) i.e. $PBNP\text{-}AgNP_1$, $PBNP\text{-}AgNP_2$ is also explored as shown in Table 1. The results justify better catalytic activity of $PBNP\text{-}AgNP_2$ and confirm the role of organic-inorganic hybrid as relatively higher concentration of 3-APTMS is required during the synthesis of $AgNP_2$ as compared to that of $AgNP_1$ (Supporting information S1).

Further bimetallic nanoparticles made from Ag/Au ratio of 1/4 was used to make PBNP-Au-Ag nanocomposite for such catalytic measurement as shown in visual photographs (Figure 9a) in order to calculate the Michaelis-Menten constant (K_m) and maximal reaction velocity (V_{max}). The results on catalytic activity are recorded in Table 1. Our results revealed better catalytic behaviour of PBNP-Au-Ag nanocomposite as compared to others PBNP, $PBNP\text{-}AgNP_1$, $PBNP\text{-}AgNP_2$ (Table 1). Typical results for PBNP-Au-Ag nanocomposite are shown in Figure 9b. The nanocomposite is efficient to probe glucose oxidase catalyzed reaction with excellent sensitivity on glucose analysis (data not shown).

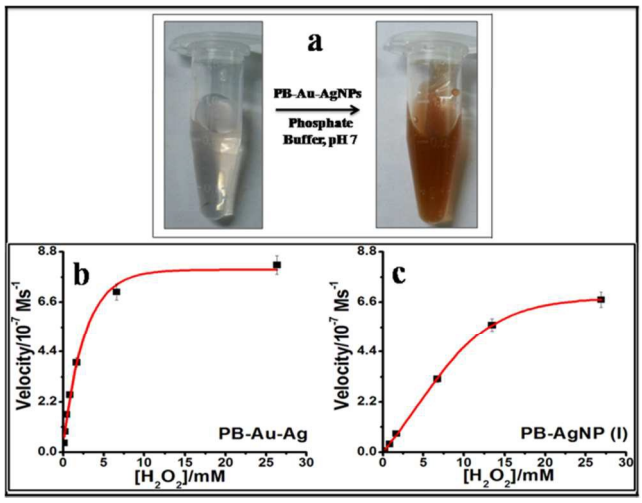

Fig. 9 (a) Colour evaluation upon addition of PBNP-Au-AgNPs to *o*-dianisidine-H_2O_2 system; **(b)** Kinetic analysis for PBNP-Au-AgNPs with *o*-dianisidine as substrates; **(c)** Kinetic analysis for PBNP-AgNP (I) with *o*-dianisidine as substrates in phosphate buffer.

The best k_m to the order of 1.7 mM is recorded for PBNP-Au-Ag nanocomposite representing better catalytic behaviour than that of peroxidase recorded to 3.7 mM under experimental

condition[63,64] prevailing for controlling the nanoparticle/enzyme concentrations to record reliable optical measurement. The replacement of cyclohexanone by GPTMS resulting in less tuned nanocomposite formation and yield high K_m value to the order of 6.6 mM (Figure 9c, Table 1) and reveals the significance of processable Prussian blue and AgNPs/Au-Ag NPs for nanocomposite formation. The kinetic parameters support that the present nanocomposite may be a candidate of perfect peroxidase replacement for biomedical applications. It should be noted that K_m is recorded keeping similar concentrations of nanomaterials during catalytic measurement. In addition to that the presence of 3-APTMS may also encourage selective binding of receptor protein through Schiff-base/carbodiimide coupling facilitating the possibility of present material for better clinical applications.

Electrocatalytic ability of Nanocomposite. Apart from homogeneous catalytic applications of as synthesized nanocomposite, the finding on heterogeneous catalysis has also been explored. The PBNP-AgNP (I) nanocomposite are used to make a chemically modified electrode for evaluating the electrocatalysis ability of the material. The presence of AgNP (I) with PBNP enable improvement in electrochemical behaviour as shown in Figure 10A with respect to cathodic and anodic peak potential separation.

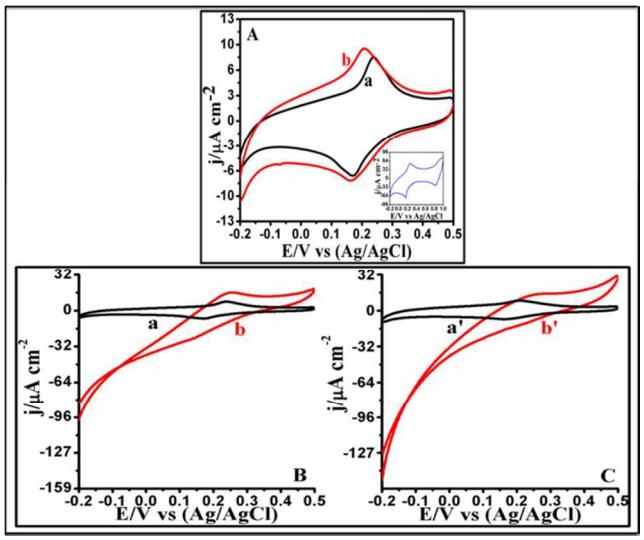

Fig. 10 (A) Cyclic voltammograms of PBNPs (a) and PBNP-AgNP (I) (b), in 0.1 M KNO_3 at scan rate of $0.01Vs^{-1}$.Cyclic voltammograms of PBNPs (B) and PBNP-AgNP (I) (C) in absence (a, a') and the presence of 5mM H_2O_2 (b, b') at the scan rate of $0.01Vs^{-1}$ in 0.1 M phosphate buffer (pH 7.0) containing 0.5 M KCl.

The electrochemical behaviour of nanocomposite between -0.2 to 1 V vs Ag/AgCl is shown in inset to Figure 10A revealing the significance of chemically synthesized PB-nanocomposite. The electrocatalytic behaviour of PBNP-AgNP (I) nanocomposite has been examined on the reduction of H_2O_2 and compared to that of the same recorded on only PBNP-modified electrode as shown in Figure 9C. H_2O_2 undergo both oxidation and reduction. The direct oxidation of the same involve large overvoltage whereas direct reduction of H_2O_2 start at 0 V vs Ag/AgCl and dynamics of such reduction increases with an increase in cathodic potential.[65] Catalytic reduction, as shown in Figure 10 B and C, start close to the redox potential of PB and subsequently follow similar trend as observed in direct reduction. The use of Horseradish

peroxidase (HRP) also facilitate the reduction of H_2O_2 at slightly anodic potential and dynamics of the same increases with an increase of operating potential in cathodic direction [65] similar to that as recorded in Figure 10 B and C.

Table 1
Kinetic parameters for the peroxidase-like activity of PBNP-AgNP and PBNP-Au-Ag nanocomposite.

S No.	Catalyst	Substrate	K_m/mM	V_{max}/ms^{-1}
1.	PBNP	H_2O_2	9.04	$8.40x10^{-7}$
2.	PBNP-$AgNP_1$	H_2O_2	3.32	$3.15x10^{-7}$
3.	PBNP-$AgNP_2$	H_2O_2	2.05	$4.15x10^{-7}$
4.	PBNP-Au-Ag	H_2O_2	1.7	$7.82x10^{-7}$
5.	PBNP-AgNP(I)	H_2O_2	6.6	$6.30x10^{-7}$
6.	HRP[63,64]	H_2O_2	3.7	$8.71x10^{-8}$

The results based on voltammetry for (B) PBNP and (C) PBNP-AgNP (I) systems in absence (a, a') and the presence (b, b') of 5 mM H_2O_2 confirm the better catalytic behaviour of PBNP-AgNP(I) electrode system. The finding confirms enhanced electrocatalytic activity of nanocomposite as compared to that of only PBNP on H_2O_2 analysis. Again the modified electrode is suitable material for electrochemical probing of many oxidase catalyzed reaction coupled in a flow injection system presenting the wider application of nanocomposite modified electrode for efficient detection of H_2O_2 generated in enzymatic packed bed reactor.[66]

Conclusions

A facile method for the synthesis of functional AgNPs and bimetallic Au-Ag NPs are reported representing major contribution of organic reducing agents i.e. formaldehyde and cyclohexanone and micellar behaviour of 3-APTMS. The use of similar reducing agents also enables the synthesis of polycrystalline PBNPs that allow the formation of nano-structured composites of a crystallized framework. In addition to that the suitable composition of 3-APTMS and organic reducing agents not only control the dispersibility in variety of solvents but also enable the formation of organic-inorganic hybrid that facilitated catalytic activity of as synthesized nanomaterials. The finding also demonstrates the requirement of suitable composition of nanoparticles that can be tuned for nanocomposite formation for better catalytic activity with wider applications in both homogeneous and heterogeneous catalysis. With the example of AgNPs, Ag-Au and nanocomposite of PBNPs, tailoring of peroxidase-like activity justifying another effective way to regulate the synthesis and catalytic activity of NPs is reported.

Acknowledgements

The authors are thankful to UGC for one time research grant and IIT (BHU) for the award of TAship. Ms. Bharathi and Mr. Amit, of SAIF, IIT, Mumbai are greatly acknowledged for providing their valuable support on TEM analysis.

References

1 L. K. Kelly, E. Coronado, L. L. Zhao and G. C. Schatz, *J. Phys. Chem. B*., 2003, **107**, 668-677.

2 D. D. Evanoff and G. Chumanov, *ChemPhysChem.* 2005, **6**, 1221-1231.

3 J. Wu, L. H. Tan,K. Hwang, H. Xing, P. Wu, W. Li and Y. Lu, *J. Am. Chem. Soc.* 2014, **136**, 15195-15202.

4 Q. linand Z. Sun, *J. Phys. Chem. C*. 2011, **115**, 1474-1479.

5 A. Panacek, R. Prucek, J. Hrbac, T. Nevecena, J. Steffcova, R. Zboril and L. Kvitek, *Chem. Mater.* 2014, **26**, 1332-1339.

6 B. Baruah, G. J. Gabriel, M. J. Akbashev and M. E. Booher, *Langmuir*, 2013, **29**, 4225-4234.

7 A. Panacek, L. Kvitek, R. Prucek, M. Kolar, R. Vecerova, N. Pizurova, V. K. Sharma, T. Nevecna and R. Zboril, *J. Phys. Chem. B.* 2006, **110**, 16248-16253.

8 L. Rizzello and P. P. Pompa, *Chem. Soc. Rev*. 2014, **43**, 1501-1518.

9 A. Niu, Y. Han, J. Wu, N. Yu and Q. Xu, *J. Phys. Chem. C.,* 2010, **114**, 12728-12735.

10 Y. Sun and Y. Xia, *Science,* 2002, **298**, 2176-2179.

11 Y. Li, Y. Wu and B. S. Ong, *J. Am. Chem. Soc,* 2005, **127**, 3266-3267.

12 S. Chernousova and M. Epple, *Angew. Chem., Int. Ed.* 2013,**52**, 1636–1653.

13 L. Lu, H. Wang, Y. Zhou, S. Xi, H. Zhang, J. Hu and B. Zhao,*Chem. Commun*., 2002, 144-145.

14 Z. Y.Li, J. Yuan, Y. Chen, R. E. Palmer and J. P. Wilcoxon, *Adv. Mater*. 2005, **17**, 2885-2888.

15 R. Ferrando, J. Jellinek and R. L. Johnston,*Chem. Rev*. 2008, **108**, 845-910.

16 L. L. Lazarus, C. T. Riche, B. C. Marin, M. Gupta, N. Malmstadt and R. L. Brutchery, *ACS Appl. Mater. Interfaces*., 2012, **4**, 3077-3083.

17 Y. Bu and S. Lee, *ACS Appl. Mater. Interfaces.* 2012, **4**, 3923-3931.

18 C. H. Li, A. C. Jamison, S. Rittikulsittichai, T. C. Lee and T. R. Lee, *ACS Appl. Mater. Interfaces*, 2014, **6**, 19943-19950.

19 M. Sharma, P. R. Pudasaini, F. R. Zepeda, E. Vinogradova and A. A. Ayon, *ACS Appl. Mater. Interfaces,* 2014, **6**, 15472-15479.

20 J. Sun, F. Yang, D. Zhao, C. Chen and X. Yang, *ACS Appl.Mater.Interfaces*.2015, **7**, 6860-6866.

21 J. Shi, *Chem. Rev*. 2013, **113**, 2139−2181.

22 S. K. Bhargava, J. M. Booth, S. Agrawal, P. Coloe and G. Kar, *Langmuir*, 2005, **21**, 5949-5956.

23 J. D. S. Newman and G. J. Blanchard, *Langmuir* 2006, **22**, 5882-5887.

24 P. C. Pandey and G. Pandey, *J.Nanosci. Nanotechnol.*doi:10.1166/jnn.2015.11104.

25 T. Sainsbury, T. Ikuno, D. Okawa, D. Pacile, J. M. J. Frechet and A.Zettl, *J. Phys. Chem. C.,* 2007, **111**, 12992-12999.

26 P. C. Pandey and D. S. Chauhan, *Analyst,* 2012, **137**, 376-385.

27 P. C. Pandey, A. K.Pandey and G. Pandey, *J. Nanosci. Nanotechnol.* 2014, **14**, 6606-6613.

28 P. C. Pandey and G. Pandey,*J. Mater. Chem. B.* 2014, **2**, 3383-3390.

29 P. C. Pandey, R. Singh and A. K. Pandey, *Electrochim. Acta*. 2014, **138**, 163-173.

30 P. C. Pandey and R. Singh, *RSC Adv*. 2015, **5**, 10964-10973.

31 P. C. Pandey, D. Panday and G. Pandey, *RSC Adv*. 2014, **4**, 60563-60572.

32 P. C. Pandey and A. K. Pandey, *Electrochim. Acta.* 2013, **87**, 1-8.

33 P. C. Pandey and A. K. Pandey, *Analyst*, 2013, **138**, 2295-2301.

34 H. Wei and E. Wang, *Anal. Chem*. 2008, **80**, 2250-2254.

35 Y. Jv, B. Li and R. Cao, *Chem. Commun*. 2010, **46**, 8017-8019.

36 H. Jiang, Z. Chen, H. Cao and Y. Huang, *Analyst*, 2012, **137**, 5560-5564.

37 L. Zhang, L. Han, P. Hu, L. Wang and S. Dong, *Chem. Commun*., 2013, **49**, 10480-10482.

38 W. He, X. Wu, J. Liu, X. Hu, K. Zhang, S. Hou,W. Zhou and S. Xie, *Chem.Mater*., 2010, **22**, 2988-2994.

39 N. A. Sitnikova, M. A. Komkova, I. V. Khomyakova, E. E. Karyakina and A. Karyakin, *Anal. Chem*., 2014, **86**,4131 −4134.

40 N. R. Tacconi and K. Rajeshwar, *Chem. Mater*.2003, **15**, 3046-3062.

41 A. A. Karyakin, E. A. Puganova, I. A. Budashov, I. N. Kurochkin, E. E. Karyakina, E. E.; V. A. Levchenko, V. N. Matveyenko and S. D. Varfolomeyev, *Anal.Chem*. 2004, **76**, 474-478.

42 P. C. Pandey and R. Singh, *J. Nanosci. Nanotechnol,* 2015, **15**, 5749-5759.

43 B. L. Cushing, V. L. Kolesnichenko and C. J. Connor, *Chem. Rev*, 2004, **104**, 3893-3946.

44 M. C. Daniel and D. Astruc, *Chem. Rev*, 2004, **104**,293-346.

45 S. Kango, S. Kalia, A. Celli, J. Njuguna, Y. Habibi and R. Kumar, *Prog. Polym. Sci.* 2013, **38**, 1232-1261.

46 R. G. Chaudhari and S. Paria, *Chem. Rev*. 2012, **112**, 2373-2433.

47 A. P. Wight and M. E. Davis, *Chem. Rev*. 2002, **102**, 3589-3614.

48 Y. B. Tewari, M. M. Schantz, P. C. Pandey, M. V. Rekharsky and R. N. Goldberg, *J. Phys.Chem.* 1995, **99**, 1594-1601.

49 H. H. Weetall, *Appl.Biochem. Biotechnol*., 1993, **41**, 157-188.

50 Y. N. Wong, N. J. Boonton, U. S. Patent, 5,601, 979, 1997.

51 P. C. Pandey, S. Upadhyay and H. C. Pathak, *Electroanalysis,* 1999, **11**, 59-65.

52 P. C. Pandey, S. Upadhyay, H. C. Pathak, I. Tiwari and V. S. Tripathi, *Electroanalysis,* 1999, **11**, 1251-1258.

53 P. C .Pandey, S. Upadhyay and H. C. Pathak, *Sens. Actuators. B*., 1999, **60**, 83-89.

54 P. C. Pandey, S. Upadhyay, N. K. Shukla and S. Sharma, *Biosens. Bioelectron.,* 2003, **18**, 1257-1268.

55 P. C. Pandey and B. Singh, *Biosens. Bioelectron.,* 2008, **24**, 842-848.

56 P. C. Pandey and S. Upadhyay, *Sens. Actuators. B.,* 2001, **78**, 148-155.

57 P. C. Pandey, S. Upadhyay and S. Sharma, *J. Electrochem. Soc.,* 2003, **150**, H85-H92.

58 P. C. Pandey and A. Prakash, *J. of Electroanal. Chem.,* 2014, **729**, 95-102.

59 C. M. Gonzalez, Y. Liu and J. C. Scaiano, *J. Phys.Chem. C.,* 2009, **113**, 11861-11867.

60 P. Bayliss, D. C. Erd, M. E. Mrose, A. P. Sabina and D. K. Smith, *Mineral Powder Diffraction FileData Book JCPDS,* 1986.

61 H. Chen, Y. Li, F. Zhang, G. Zhang, X. Fan and *J. Mater. Chem*., 2011, **21**, 17658-17661.

62 T. Arun, R. Prakash and J. Joseyphus, *J. Magn. Magn. Mater*. 2013, **345**, 100-105.

63 L. Gao, J. Zhuang, L. Nie, J. Zhang, Y. Zhang, N. Gu, T. Wang, J. Feng, D. Yang, S. Perrett and X. Yan, *Nat. Nanotechnol*. 2007, **2**, 577-583.

64 X. Q. Zhang, S. W. Gong, Y. Zhang, T. Yang, C. Y. Wang and N. Gu, *J. Mater. Chem*., 2010, **20**, 5110-5116.

65 P. C. Pandey, S. Upadhyay, I. Tiwari and V. S. Tripathi, *Sens. Actuators*. 2001, **72**, 224-232.

66 P. C. Pandey and H. H. Weetall, *Anal. Biochem*., 1995, **224**, 428-433.

Preparation and Characterization of Ag, Ag-Au/Au-Ag nanoparticles and its nanocomposite with Prussian blue for bioanalytical applications

Prem. C. Pandey, Richa. Singh and Yashashwa Pandey,

Department of Chemistry, Indian Institute of Technology (BHU), Varanasi-221005, UP, India.
E-mail: pcpandey.apc@iitbhu.ac.in

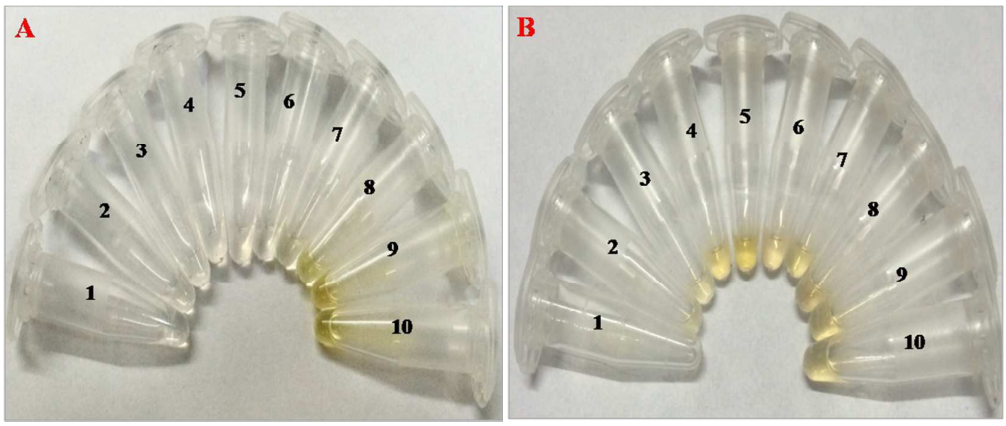

Figure S1. Formation of AgNPs as a function of; (A) 3-APTMS concentrations (Table S1A, Sr. no. 1 to 10) and (B) Cyclohexanone concentrations (Table S1B, Sr. no. 1 to 10): keeping constant concentrations of cyclohexanone/3-APTMS (1.9 M/0.5 M) and 0.01 M $AgNO_3$.

Table S1 (A)

Characteristics of different Silver nanoparticles (AgNPs) made from Cyclohexanone as a function of 3-APTMS concentration.

Sr. no.	$AgNO_3$ (M)	3-APTMS (M)	Cyclohexanone (M)	AgNPs formation	Extent of formation
1	0.01	$0.1x10^{-3}$	1.9	White	-
2	0.01	0.001	1.9	White	-
3	0.01	0.005	1.9	White	-
4	0.01	0.01	1.9	White	-
5	0.01	0.05	1.9	White	-
6	0.01	0.1	1.9	White	-
7	0.01	0.25	1.9	Light Yellow($AgNP_1$)	++
8	0.01	0.5	1.9	Yellow($AgNP_2$)	++++
9	0.01	1	1.9	Yellow	++++
10	0.01	2	1.9	Yellow	++++

"-" sign represents that the AgNPs are not formed whereas number of "+" sign denotes the relative rate of AgNPs formation.

Table S1 (B)

Characteristics of different Silver nanoparticles (AgNPs) as a function of Cyclohexanone concentration.

S. no.	$AgNO_3$ (M)	3-APTMS (M)	Cyclohexanone (M)	AgNPs formation	Extent of formation
1	0.01	0.5	0.3	White	-
2	0.01	0.5	0.6	White	-
3	0.01	0.5	0.9	Light Yellow	+
4	0.01	0.5	1.4	Light Yellow	++
5	0.01	0.5	1.9	Dark Yellow	++++
6	0.01	0.5	2.4	Light Yellow	+++
7	0.01	0.5	2.8	Light Yellow	+++
8	0.01	0.5	3.2	Light Yellow	+++
9	0.01	0.5	3.5	Light Yellow	+++
10	0.01	0.5	3.8	Light Yellow	+++

"-" sign represents that the AgNPs are not formed whereas number of "+" sign denotes the relative rate of AgNPs formation.

Figure S1. Formation of AgNPs as a function of: (C) 3-APTMS concentrations (Table S1C, Sr. no. a to j) keeping constant concentrations of Formaldehyde (0.8 M) and 0.01 M $AgNO_3$.

Table S1 (C) Characteristics of different Silver nanoparticles (AgNPs) made from Formaldehyde as a function of 3-APTMS concentration.

Sr. no.	$AgNO_3$ (M)	3-APTMS (M)	Formaldehyde (M)	AgNPs formation	Extent of formation
a	0.01	$0.1x10^{-3}$	0.8	White	-
b	0.01	0.001	0.8	White	-
c	0.01	0.005	0.8	White	-
d	0.01	0.01	0.8	White	-
e	0.01	0.05	0.8	Grey	-
f	0.01	0.1	0.8	Dark Grey	-
g	0.01	0.25	0.8	Light Yellow	+++
h	0.01	0.5	0.8	Yellow	+++
i	0.01	1	0.8	Yellow	++++
j	0.01	2	0.8	Dark Yellow	++++

"-" sign represents that the AgNPs are not formed whereas number of "+" sign denotes the relative rate of AgNPs formation.

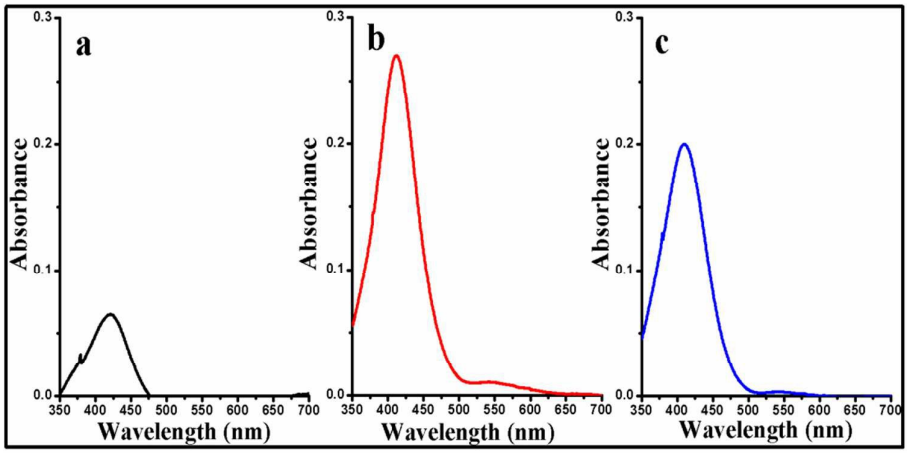

Figure S1 (D) Effect of Formaldehyde concentrations on the formation of AgNPs [(a) 0.4 M, (b) 0.8 M and (c) 1.2 M] keeping constant concentration of 3-APTMS (0.5 M).

Supporting Information S2.

Cyclohexanone in the prevailing medium undergoes keto– enol tautomerism. Enolate ion acts as an electron donor to 3-APTMS capped Ag^{+} ion, which in turn acts as a Lewis acid, leading to the formation of AgNPs along with organic-inorganic hybrid (Scheme-1) and has been confirmed by FTIR spectroscopy. The broad band between 3800 and 2800 cm^{-1} is related to the overlap of O-H vibration modes with the organic modes. The IR peaks at 1090-1120 cm^{-1} due to the vibrations of the C-Si-O group. A series of bands at around 2820-2940 cm^{-1} due to the vibrations of methylene $-(CH_2)_3-$ and the peaks at about 1220-1275 cm^{-1} are due to the vibrations of $Si-CH_3$.

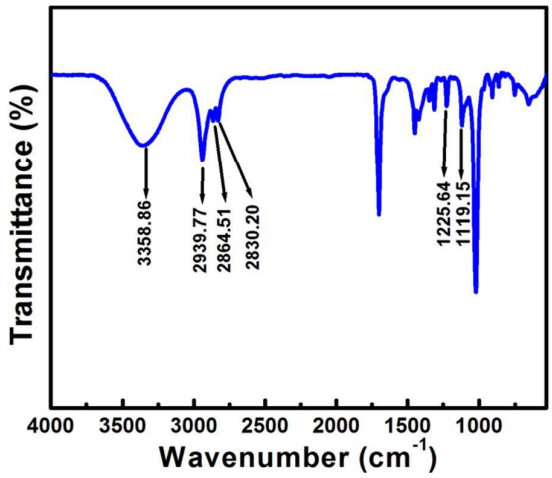

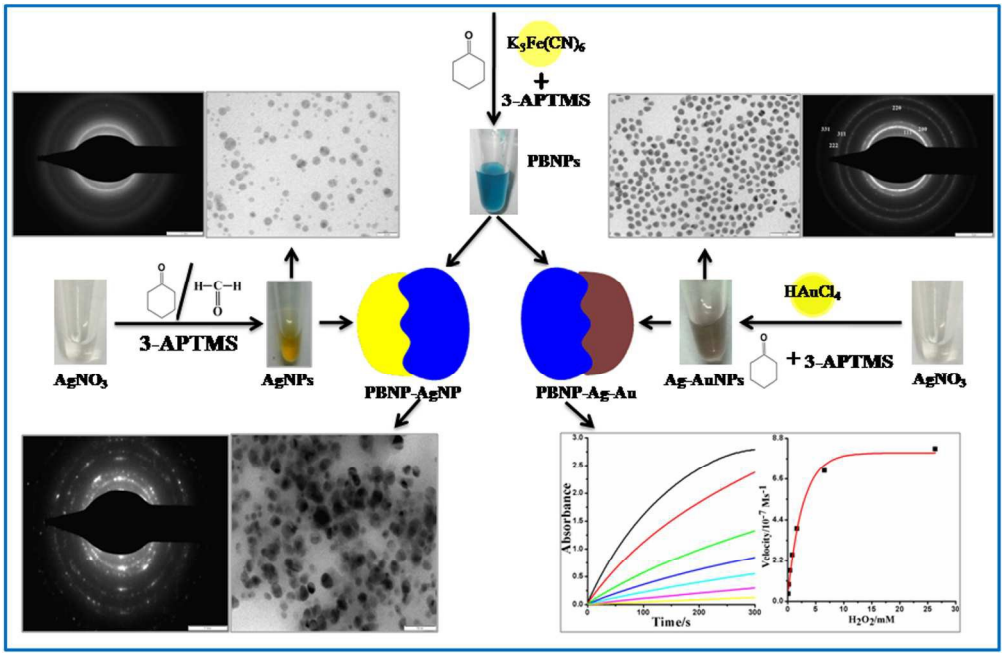

A facile method for the synthesis of functional AgNPs and bimetallic Ag-Au/Au-Ag are reported enabling the formation of nanocomposite with Prussian blue in a crystalline framework for bioanalytical applications, involving active role of organic reducing agents and 3-aminopropyltrimethoxysilane.
266x172mm (300 x 300 DPI)